Neuron
Article

Identification of an Inhibitory Circuit that Regulates Cerebellar Golgi Cell Activity

Court Hull[1] and Wade G. Regehr[1,*]
[1]Department of Neurobiology, Harvard Medical School, Boston, MA 02115, USA
*Correspondence: wade_regehr@hms.harvard.edu
DOI 10.1016/j.neuron.2011.10.030

SUMMARY

Here we provide evidence that revises the inhibitory circuit diagram of the cerebellar cortex. It was previously thought that Golgi cells, interneurons that are the sole source of inhibition onto granule cells, were exclusively coupled via gap junctions. Moreover, Golgi cells were believed to receive GABAergic inhibition from molecular layer interneurons (MLIs). Here we challenge these views by optogenetically activating the cerebellar circuitry to determine the timing and pharmacology of inhibition onto Golgi cells and by performing paired recordings to directly assess synaptic connectivity. In contrast to current thought, we find that Golgi cells, not MLIs, make inhibitory GABAergic synapses onto other Golgi cells. As a result, MLI feedback does not regulate the Golgi cell network, and Golgi cells are inhibited approximately 2 ms before Purkinje cells, following a mossy fiber input. Hence, Golgi cells and Purkinje cells receive unique sources of inhibition and can differentially process shared granule cell inputs.

INTRODUCTION

The cerebellar cortex plays a crucial role in orchestrating the coordination and timing of body movements (Mauk et al., 2000), and cerebellar deficits or damage typically results in severe ataxia (Grüsser-Cornehls and Bäurle, 2001). At the neural circuit level, timing is often governed by local synaptic inhibition, which is critical for regulating spike timing, population synchrony, and the frequency and amplitude of neural oscillations (Atallah and Scanziani, 2009; Cobb et al., 1995; Mann et al., 2005; Pouille and Scanziani, 2001).

In the cerebellar cortex, inhibition is provided by only a few distinct types of interneurons (Eccles et al., 1966), and the general consensus is that all major pathways of synaptic inhibition have been identified. Of particular importance for local synaptic processing is the cerebellar Golgi cell (D'Angelo, 2008). This interneuron is positioned in the granule cell layer at the input stage of the cerebellar cortex (Figure 1A). Here, sensory, motor, and higher cognitive information from several brain regions carried by the mossy fibers (MFs), provides strong excitatory drive to both Golgi cells and glutamatergic granule cells (Eccles et al., 1967; Ito, 2006). In turn, Golgi cells generate the sole source of inhibition onto granule cells (Eccles et al., 1964), which are the most numerous cell type in the brain. Golgi cells can also directly inhibit release from MFs by activating presynaptic $GABA_B$ receptors (Mitchell and Silver, 2000). Hence, by regulating the excitability of both granule cells and MFs, Golgi cells can gate sensory activation of the cerebellar cortex and thus have a major impact on cerebellar processing (Galliano et al., 2010).

Golgi cells have indeed been found to play an integral role in cerebellar function. At the behavioral level, acute ablation of Golgi cells results in ataxia (Watanabe et al., 1998). Moreover, Golgi cells are essential for generating behaviorally important temporal patterns of activity in the cerebellum (De Schutter et al., 2000; Isope et al., 2002; Kistler and De Zeeuw, 2003). Electrical connections between Golgi cells, which are mediated by gap junctions on their dendrites, allow both synchronous Golgi cell spiking during periods of quiet wakefulness (Dugué et al., 2009) and desynchronized spiking in response to MF activation (Vervaeke et al., 2010).

To understand how Golgi cells make such essential contributions to local cerebellar processing, it is necessary to understand how their activity is regulated by synaptic inhibition. Some of the inhibition onto Golgi cells is generated by rare interneurons called Lugaro cells, which provide a mixed glycinergic/GABAergic input (Dumoulin et al., 2001). However, this input has only been observed in vitro in the presence of serotonin (Dieudonné and Dumoulin, 2000) and does not account for the more prominent GABAergic inhibition of Golgi cells. Indirect evidence, both anatomical (Palay and Chan-Palay, 1974) and physiological (Dumoulin et al., 2001), has suggested that molecular layer interneurons (MLIs) inhibit Golgi cells in the same manner as Purkinje cells (PCs) and may also be electrically coupled to Golgi cells via gap junctions (Sotelo and Llinás, 1972). Because recent studies have failed to identify inhibitory synaptic connections between Golgi cells (Dugué et al., 2009; Vervaeke et al., 2010), the prevailing view maintains that the Golgi cell network is connected exclusively by gap junctions and receives GABAergic inhibition from MLIs (Geurts et al., 2003; D'Angelo and De Zeeuw, 2009; De Schutter et al., 2000; Isope et al., 2002; Galliano et al., 2010; Jörntell et al., 2010). This longstanding hypothesis suggests an important functional role for MLIs in providing ongoing feedback inhibition to Golgi cells and hence in regulating activity throughout the granule cell layer.

Here, we overturn this view by revealing that Golgi cells make inhibitory GABAergic synapses onto each other and do

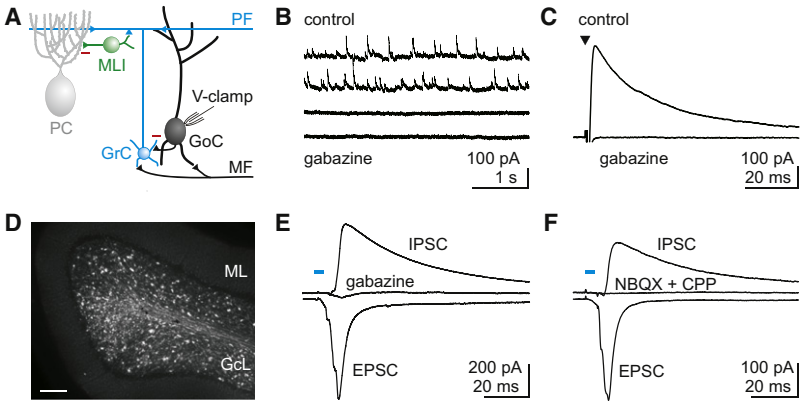

Figure 1. GABAergic Inhibitory Inputs to Golgi Cells

(A) Schematic showing the major cell types in the cerebellar cortex with their known synaptic contacts. Abbreviations as follows: PC, Purkinje cell; PF, parallel fiber; MLI, molecular layer interneuron; GrC, granule cell; GoC, Golgi cell; MF, mossy fiber; V-clamp, voltage clamp. Inhibitory synapses (red minus sign) and all other synapses (triangles) are glutamatergic.

(B) Spontaneous inhibitory postsynaptic currents recorded from Golgi cells at a holding potential of +10mV in the presence of NBQX (5 μM) and CPP (2.5 μM) to block glutamatergic inputs. All events were blocked by the $GABA_AR$ antagonist gabazine (5 μM).

(C) Average IPSC evoked with a stimulus electrode placed in the granule cell layer near the recorded Golgi cell. Evoked IPSCs were also blocked by gabazine.

(D) Fluorescence image of a cerebellar slice from the vermis of a Thy1-ChR2/EYFP mouse that expresses channelrhodopsin 2 (ChR2) and YFP in a subset of MFs. GcL, granule cell layer; ML, molecular layer. Scale bar represents 100 μm.

(E) Optical stimulation of ChR2-expressing MFs (473 nm light for 5 ms) evoked EPSCs (recorded at the reversal potential for IPSCs; see Experimental Procedures) and IPSCs (recorded at the EPSC reversal potential). IPSCs evoked by ChR2 activation were blocked by gabazine.

(F) In another experiment, ChR2-evoked IPSCs were also abolished by blocking glutamatergic transmission (NBQX and CPP), indicating that they were polysynaptic.

not receive either inhibitory synapses or electrical connections from MLIs. This indicates that a significant revision of the inhibitory wiring diagram of the cerebellar cortex is needed. Moreover, these newfound connections have functional implications for the timing of inhibition onto Golgi cells, for how these cells are activated, and ultimately for how they regulate MF excitation of the cerebellar cortex.

RESULTS

Golgi cells are known to receive robust GABAergic inhibitory inputs (Dumoulin et al., 2001). Through the use of whole-cell voltage-clamp recordings, we find that Golgi cells in cerebellar slices receive a continuous barrage of spontaneous GABAergic inhibitory postsynaptic currents (IPSCs) that are blocked by the $GABA_A$ receptor antagonist gabazine (6.4 ± 1.0 Hz in control and 0.13 ± 0.03 Hz in gabazine, 5 μM, n = 6; Figure 1B). Furthermore, large IPSCs are readily evoked with an extracellular stimulus electrode placed in the granule cell layer near Golgi cell somata (362 ± 51 pA, n = 20; Figure 1C). These IPSCs are predominantly GABAergic and are abolished by gabazine (3% ± 1% of control, n = 19). In one additional cell, a large strychnine-sensitive glycinergic component of inhibition was also apparent (Figure S1A). Hence, all spontaneous inhibition and the vast majority of electrically evoked inhibitory input to Golgi cells are GABAergic. Although the spontaneous IPSCs onto Golgi cells suggest that tonically active neurons inhibit Golgi cells, this property cannot be used to identify the source of their inhibition, because both MLIs and Golgi cells are spontaneously active.

To explore the source of Golgi cell inhibition, we took advantage of the intact circuitry of a cerebellar brain slice to activate inhibition with a known excitatory input. Hence, an optogenetic approach was used to selectively activate MFs in transgenic mice (Thy1-ChR2/EYFP line 18) that express channelrhodopsin 2 (ChR2) and yellow fluorescent protein (YFP) in a fraction of cerebellar MFs (Figure 1D; Figure S2). In these slices, a brief pulse of blue light evoked a compound excitatory postsynaptic current (EPSC) onto Golgi cells, followed with a latency of 3.1 ± 0.4 ms by a large GABAergic IPSC (control: 207 ± 50 pA,

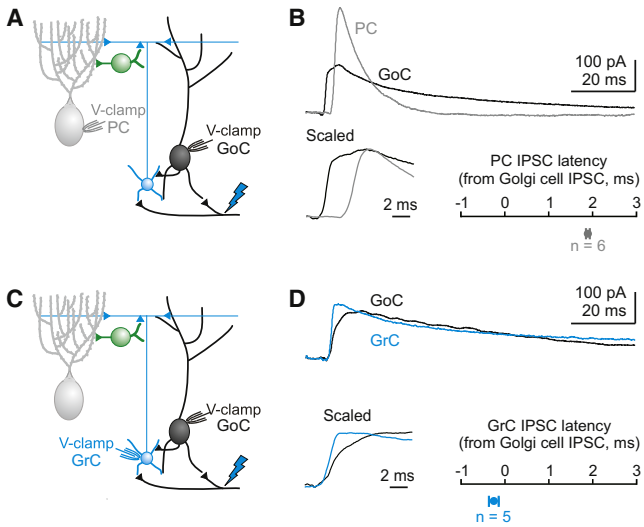

Figure 2. Timing of MF-Evoked Inhibition onto Golgi Cells, Purkinje Cells, and Granule Cells

(A) Schematic illustrating the recording configuration for (B). Blue bolt represents ChR2 activation with 473 nm light.

(B) Top: simultaneous recordings from a Purkinje cell (gray) and a Golgi cell (black) at the EPSC reversal potential demonstrate IPSCs onto both cells following ChR2 activation. Bottom left: scaled IPSCs on an expanded timescale show that the Golgi cell IPSC arrives earlier than the Purkinje cell IPSC. Bottom right: on average, Golgi cell IPSCs arrived nearly 2 ms earlier than IPSCs onto simultaneously recorded Purkinje cells (n = 6).

(C) Schematic of the recording configuration for (D).

(D) Top: simultaneous recordings of IPSCs evoked by ChR2 activation for a granule cell (blue) and a Golgi cell (black). Bottom left: scaled IPSCs on an expanded timescale show that the Golgi cell IPSC and granule cell IPSC arrive simultaneously. Bottom right: on average, for simultaneously recorded Golgi cells and granule cells, IPSCs arrived synchronously (n = 5).

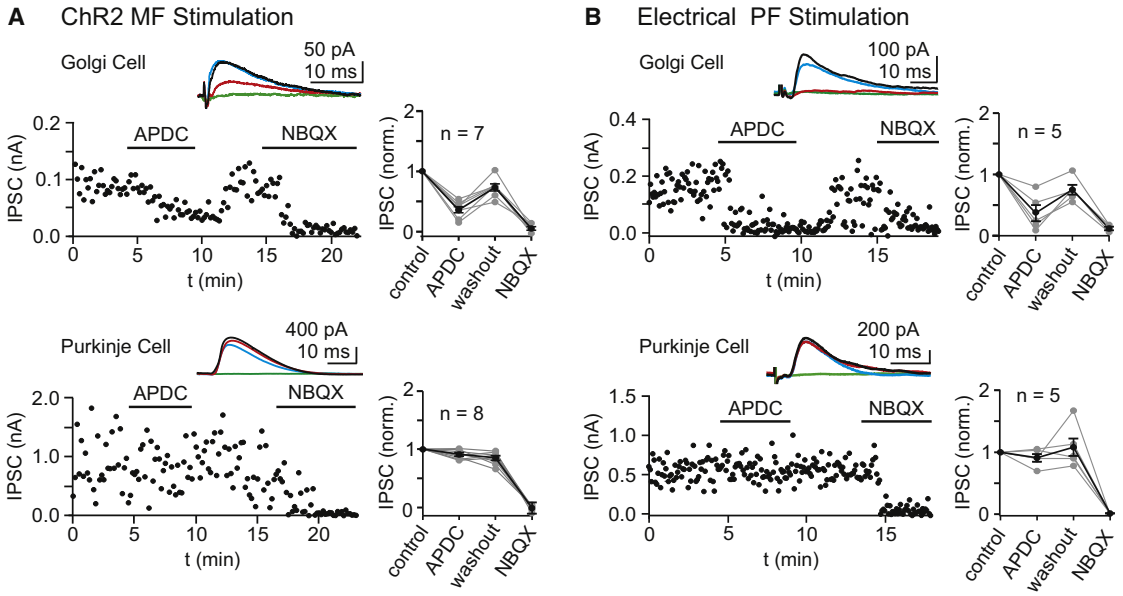

Figure 3. Differential Pharmacology IPSCs onto Golgi and Purkinje Cells Evoked by Either MF or PF Activation

Following stimulation of either MFs with light (in Thy1-ChR2/EYFP mice) (A) or PFs with an extracellular stimulus electrode (B), the resulting disynaptic IPSCs were recorded at Golgi cells and Purkinje cells, and the pharmacological sensitivity to the selective group II mGluR agonist APDC (2 μM) was measured. As shown in representative experiments for each condition (left) and in the summaries (right), Golgi cell IPSCs were strongly attenuated by APDC, but Purkinje cell IPSCs were unaffected. IPSCs in both cells were abolished by blocking glutamatergic transmission (5 μM NBQX and 2.5 μM CPP), indicating that they were disynaptic. Insets show the averaged IPSCs in control (black), APDC (red), washout (blue), and NBQX (green).

gabazine: 13 ± 6 pA, n = 6; Figure 1E). This inhibition was polysynaptic, based on the delay between EPSCs and IPSCs, and because it was eliminated by blocking AMPA and NMDA receptors (control: 140 ± 50 pA, NBQX/CPP: 7 ± 7 pA, n = 12; Figure 1F). In one case, blocking glutamatergic synapses did not abolish inhibition, and this was likely the result of a rare nonglutamatergic (Barmack et al., 1992a, 1992b; Jaarsma et al., 1997; Kerr and Bishop, 1991) activation of a glycinergic neuron (Figure S1B) (Dugué et al., 2005; Dumoulin et al., 2001). Hence, inhibition of Golgi cells following activation of the cerebellar MFs is predominantly a robust, polysynaptic input mediated by $GABA_A$ receptors.

As a first step in determining the source of GABAergic input to Golgi cells, we measured the timing of IPSCs evoked by ChR2 stimulation of the MFs. If MLIs inhibited both Golgi cells and Purkinje cells, then the onset of inhibition would likely occur at the same time in both cell types following MF activation. Surprisingly, in simultaneous recordings from Golgi cells and Purkinje cells (Figure 2A), the onset of inhibition occurs almost 2 ms earlier in Golgi cells (latency from Golgi cell IPSC to Purkinje cell IPSC = 1.9 ± 0.4 ms, n = 6, p = 0.006; Figure 2B). This time difference is inconsistent with the same population of interneurons, namely the MLIs, providing inhibition to both Golgi cells and Purkinje cells. Under these experimental conditions, inhibition of Purkinje cells involves three synapses (MF → granule cells → MLIs → Purkinje cells) (Ito, 2006). The shorter latency inhibition of Golgi cells is consistent with a disynaptic inhibition, such as MF → Golgi cell → Golgi cell.

To determine whether the evoked IPSC timing is consistent with Golgi cells inhibiting each other, we compared the timing of inhibition received by Golgi cells and granule cells, which are only inhibited by Golgi cells (Ito, 2006) (Figure 2C). Simultaneous recordings from Golgi and granule cells revealed that inhibition arrives at approximately the same time onto these two cell types following MF activation (latency from granule cell IPSC to Golgi cell IPSC = 0.3 ± 0.1 ms, p = 0.09; Figure 2D). These data are consistent with Golgi cells inhibiting both granule cells and other Golgi cells.

We further tested the hypothesis that Golgi cells are inhibited primarily by other Golgi cells by assessing the pharmacological sensitivity of inhibition onto Golgi cells and Purkinje cells. Previous studies have shown that Golgi cells are the only inhibitory cell in the cerebellar cortex to express mGluR2 and that the selective group II mGluR agonist (2*R*,4*R*)-APDC strongly hyperpolarizes Golgi cells to silence their spontaneous spiking (Ohishi et al., 1994; Watanabe and Nakanishi, 2003). This suggests that APDC should reduce disynaptic inhibition mediated by Golgi cells by making it more difficult for MF or granule cell inputs to evoke spikes. In contrast, APDC should not affect Purkinje cell inhibition, which is provided by MLIs.

We tested the effect of APDC on polysynaptic inhibition following activation of either granule cell parallel fibers (PFs) or MFs (Figure 3). In these experiments, all evoked inhibitory synaptic currents were eliminated by application of glutamate receptor antagonists, indicating that they were not a result of direct activation of interneurons. In Thy1-ChR2/EYFP mice, optical activation of MFs evoked IPSCs that were significantly reduced by APDC in Golgi cells but that were unaffected in Purkinje cells (Golgi cells: 58% ± 6% reduction of IPSC amplitude, n = 7, p < 0.001; Purkinje cells: 2% ± 3% reduction of

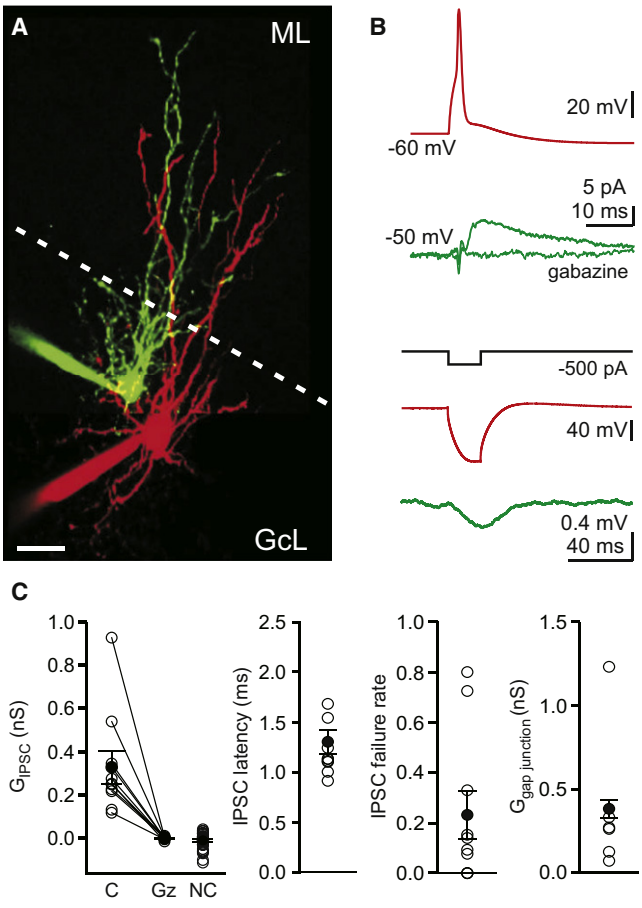

Figure 4. Paired Recordings Reveal that Golgi Cells Make GABAergic Synapses onto Each Other

(A) A pair of recorded Golgi cells filled with Alexa 488 (green) and Alexa 594 (red), imaged with two-photon microscopy. Scale bar represents 20 μm; ML, molecular layer; GcL, granule cell layer; dotted line is the boundary of the molecular layer.

(B) Experiments to test the electrical and chemical connections between neurons, with traces colored to represent the color of filled neurons in (A). Top: spiking one Golgi cell produced an IPSC in the other Golgi cell. The IPSC is the average of 30 consecutive trials, and it was blocked by gabazine. Bottom: a current step in one Golgi cell produced a large hyperpolarization in that cell and a smaller hyperpolarization in the other Golgi cell, indicating that the cells were electrically coupled.

(C) Summary data from paired recordings (50 directions, one pair = two tested directions, IPSCs were observed in 10 of 50 directions tested, three pairs reciprocally connected). Individual experiments (open circles) and averages (closed circles) are shown. Left: average conductance; middle: IPSC latency; right: IPSC failure rate and the mean gap junctional conductance. C, connected; Gz, gabazine; NC, not connected.

IPSC amplitude, n = 8, p = 0.63; Figure 3A). Similarly, through the use of a stimulus electrode to activate the PFs and recruit inhibition onto Golgi and Purkinje cells, we found that APDC selectively reduced evoked IPSCs onto Golgi cells without significantly affecting IPSCs onto Purkinje cells (Golgi cells: 54% ± 15% reduction of IPSC amplitude, n = 5, p = 0.009; Purkinje cells: 11% ± 6% reduction of IPSC amplitude, n = 5, p = 0.20; Figure 3B). This selective suppression of Golgi cell inhibition by APDC suggests that Golgi cells are inhibited by other Golgi cells rather than by MLIs.

To directly assess whether Golgi cells are synaptically inhibited by other Golgi cells, we performed paired recordings. Experiments were conducted in an external solution containing 4 mM calcium and 1 μM CGP to facilitate recording synaptic connections, because Golgi cell synapses onto granule cells can have a low release probability and may be tonically suppressed by $GABA_B$ receptors (Mapelli et al., 2009). The experimental configuration is shown in Figure 4A, and the corresponding characterization of the chemical and electrical synapses is shown in Figure 4B. These experiments revealed several unitary synaptic connections between Golgi cells (10/50 directions, 20% connected, 1 pair = 2 directions; Figure 4C). All cell pairs were imaged with two-photon microscopy and had a morphology consistent with Golgi cells. The average unitary synaptic connection between Golgi cells was 0.33 ± 0.08 nS (n = 10; Figure 4C), and three pairs were connected with reciprocal chemical synapses. Gabazine blocked these unitary synaptic currents in all cases tested (mean gabazine conductance = −0.003 nS, n = 9, p < 0.001; Figure 4C). The latency between the onset of the spike in the presynaptic cells and the IPSC was 1.3 ± 0.1 ms, and there was considerable variability in the IPSC failure rate (Figure 4C). In addition, we found that all but one of the synaptically connected pairs were also electrically coupled, which is a hallmark of Golgi cells (Dugué et al., 2009; Vervaeke et al., 2010) (gap junctional conductance = 0.38 ± 0.05 nS, n = 6; Figure 4C). Interestingly, the only pair connected chemically, but not electrically, had no dendritic overlap in the molecular layer in which gap junctions are thought to connect these cells (Vervaeke et al., 2010) (Figure S3). Importantly, we have also recorded examples of these synaptic connections in 2 mM external calcium without CGP (Figure S4). These experiments therefore provide direct evidence that Golgi cells form inhibitory GABAergic synapses onto other Golgi cells.

Can MLIs Also Regulate Golgi Cell Activity?

Although we have shown that Golgi cells inhibit each other and that the timing and pharmacology of Golgi cell inhibition is not consistent with a strong MLI→Golgi cell synaptic connection, we have not excluded the possibility that MLIs could also provide weak synaptic inhibition to Golgi cells. Because MLIs are electrically coupled to each other by gap junctions and can fire synchronously as a population, small inputs could have a large impact on Golgi cell network activity (Figure 5A). Hence, we have used dynamic clamp to determine whether weak but synchronous synaptic inhibition could regulate Golgi cell spiking.

Through the use of dynamic clamp to inject inhibitory postsynaptic conductances (IPSGs) at frequencies typical of MLI spiking (Häusser and Clark, 1997), we tested the role of weak inhibition corresponding to only a few small inputs (0.5–1 nS) on Golgi cell spontaneous spiking. As shown in a representative experiment (Figures 5B and 5C), these weak synaptic inputs delivered at 5, 10, and 15 Hz slightly decreased the Golgi cell spontaneous firing rate but strongly controlled the timing of this spiking. For 5 Hz stimulation, the Golgi cell fired out of phase with the inhibitory input. As the stimulus frequency was increased, Golgi

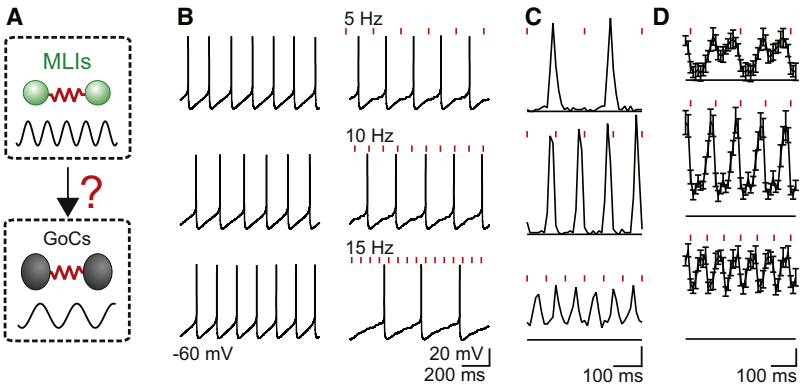

Figure 5. Golgi Cell Spiking Is Highly Sensitive to Small, Synchronous Inhibitory Inputs

(A) Schematic showing that MLIs are electrically coupled and can fire synchronously, as is the case for Golgi cells.

(B–D) Dynamic-clamp experiments were designed to test the implications of weak crossnetwork synaptic connectivity from MLIs to Golgi cells.

(B) Golgi cells were allowed to fire spontaneously at 2–8 Hz (left), and then inhibitory synaptic conductances (IPSGs, 0.5–1 nA), with the time course of inhibitory synaptic currents recorded in Golgi cells (E_{IPSG} = −75mV), were imposed at 5, 10, and 15 Hz (right) to mimic a weak inhibitory input from the MLI network.

(C) The resulting peristimulus time histograms (PSTH) for the experiment in (B) shows that inhibition from the MLI network would lead to phase locking of the Golgi cell network. Scale bar (in events/bin/stimulus) represents 0.02 in top, 0.04 in middle, and 0.06 in bottom.

(D) The average PSTH for 14 experiments also shows Golgi cell firing phase locked with its inhibitory inputs. Scale bar (in events/bin/stimulus) represents 0.01 in top, 0.02 in middle, and 0.03 in bottom. Bin widths indicate 10 ms.

cells fired less frequently than the inhibitory inputs, but the firing was still phase locked to the inhibition. Hence, even very small inhibitory inputs can reliably phase lock Golgi cell firing (Figure 5D).

These experiments suggest that Golgi cells are exquisitely sensitive to synchronous inhibitory input and that even a weak MLI→Golgi cell synaptic connection would allow the MLI network to entrain firing in the Golgi cell network. Hence, it is essential to determine whether there is any synaptic connection at all between MLIs and Golgi cells.

To test the possibility that MLIs also inhibit Golgi cells, we performed paired recordings between MLIs and Golgi cells (Figure 6A). In these experiments, we found no synaptic inputs in 124 MLI to Golgi cell pairs (61 pairs in 4 mM external calcium and 1 μM CGP and 63 pairs in 2 mM external calcium and no CGP; Figure 6B). To ensure that we could record unitary IPSCs from MLIs under our recording conditions, we performed paired recordings between MLIs and Purkinje cells (Figure 6C). In these experiments, six of ten paired recordings showed IPSCs from MLIs onto Purkinje cells (average conductance = 0.4 ± 0.1 nS, n = 6; Figure 6D). Thus, our paired recordings suggest that MLIs do not make inhibitory synapses onto Golgi cells.

Because our dynamic-clamp studies suggest that even a weak MLI→Golgi cell synapse would allow the MLI network to strongly influence the Golgi cell network, we further tested for the presence of a small MLI→Golgi cell synaptic input using a transgenic mouse line in which MLIs express ChR2 (Figure 7B; Figure S5). In these experiments, we used full-field, high-intensity light to stimulate a maximal number of MLIs while recording simultaneously from both a Golgi cell and a nearby Purkinje cell (Figure 7A). Light pulses evoked large inhibitory synaptic currents in all recorded PCs, which is consistent with the activation of many MLIs (Figures 7C and 7D; see Experimental Procedures). These synaptic responses were eliminated by the $GABA_A$-receptor antagonist gabazine. In contrast, even though many MLIs were activated in these experiments, we never observed any synaptic input onto simultaneously recorded Golgi cells (n = 6).

Previous studies have also suggested that MLIs and Golgi cells are gap junction coupled (Sotelo and Llinás, 1972). We therefore tested for such connections but found no electrical coupling between any MLIs and Golgi cells in 31 paired recordings (mean junctional conductance = −0.01 ± 0.01 nS). These experiments, along with the lack of synaptic connections observed in

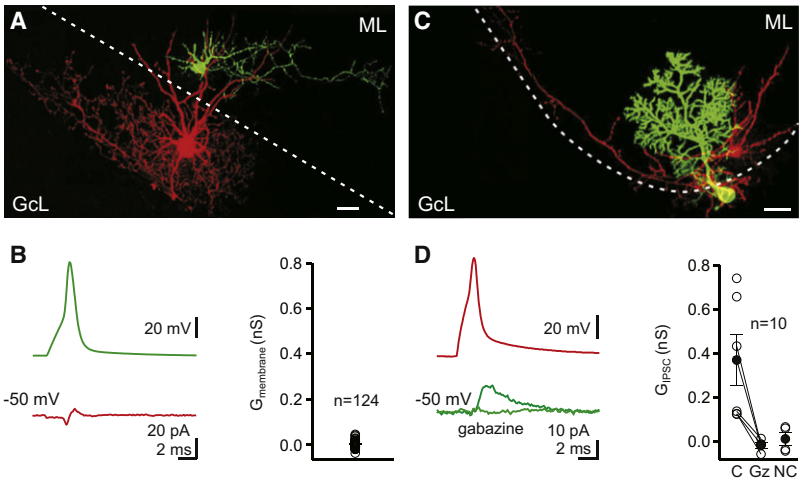

Figure 6. Paired Recordings Show No Connections between Molecular Layer Interneurons and Golgi Cells

(A) An MLI cell filled with Alexa 488 (green) and a Golgi cell filled with Alexa 594 (red), were imaged with two-photon microscopy. Scale bar represents 20 μm; ML, molecular layer; GcL, granule cell layer; dotted line is the boundary of the molecular layer.

(B) Left: spiking the MLI (green trace) did not produce an IPSC in the Golgi cell (red trace, average of 70 consecutive trials, inflection is a capacitative electrical artifact). Right: the average membrane conductance measured from 61 unconnected pairs was 0.001 nS.

(C) Paired recording from an MLI (basket cell, red) and a Purkinje cell (green).

(D) Left: spiking the MLI produced an IPSC in the Purkinje cell that was abolished by gabazine (5 μM). Right: IPSCs were observed in six of ten paired recordings between MLIs and Purkinje cells. C, connected; Gz, gabazine; NC, not connected.

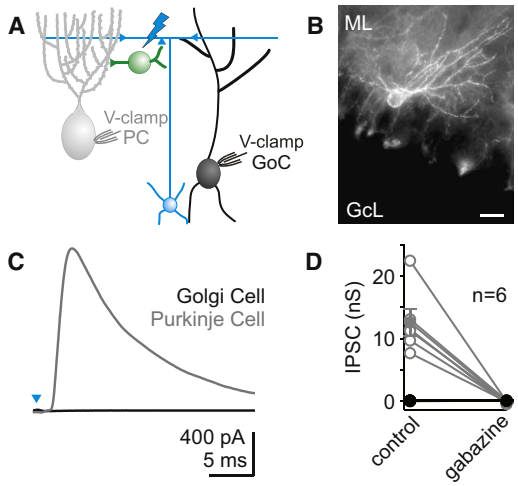

Figure 7. Transgenic Mice Expressing ChR2 in MLIs Demonstrate a Lack of Fast Inhibitory Synapses onto Golgi Cells

(A) Schematic depicting the paired whole-cell recordings of light-activated currents made simultaneously from a Golgi cell and a Purkinje cell in Prv-mhChR2/EYFP mice.

(B) A fluorescence image shows intense YFP fluorescence in MLIs. Scale bar represents 20 μm.

(C) Example of a light-evoked IPSC recorded from a Purkinje cell, with no evoked current in a simultaneously recorded Golgi cell.

(D) Six such experiments are summarized for Purkinje cells (gray) and Golgi cells (black). No currents were evoked in any Golgi cells, and currents in Purkinje cells (mean conductance = 12.6 nS) were completely blocked by the $GABA_A$ receptor antagonist gabazine.

paired recordings and with ChR2 stimulation, suggest that despite the many MLIs in the molecular layer in close proximity to Golgi cell dendrites, MLIs do not make fast inhibitory synapses or gap junctional connections onto Golgi cells.

Functional Consequences of Golgi-Cell-to-Golgi-Cell Inhibition

These findings change the inhibitory wiring diagram of the cerebellar cortex by establishing that Golgi cells are inhibited by other Golgi cells and not by MLIs (Figure 8A), but what are the consequences of this circuit revision? MF activation evokes IPSCs that arrive earlier onto Golgi cells than onto Purkinje cells (Figure 2). To determine the implications for Golgi cell activity, we examined the timing of inhibition relative to excitation in these cells. MF activation should excite Golgi cells directly (MF → Golgi cell) as well as indirectly by activating granule cell synapses (MF → granule cell → Golgi cell). Indeed, we find that brief, high-intensity optical stimulation of MFs can evoke EPSCs onto Golgi cells that consist of two discrete components (Figure 8B). Through the use the CB1 receptor agonist WIN 55,212-2 (WIN), which is known to suppress release from granule cells onto Golgi cells (Beierlein et al., 2007), we found a selective reduction of the second component of the EPSC following ChR2 activation (EPSC1: 2% ± 4% reduction, $p = 0.79$; EPSC2: 43% ± 6% reduction, $p < 0.001$, $n = 7$; Figures 8B and 8C). The observed delay between EPSC1 and EPSC2 and the pharmacological sensitivity of EPSC2 establishes that the second component of the EPSC is a result of disynaptically activating granule cell synapses.

We then compared the relative timing of evoked IPSCs and EPSCs. These experiments revealed that disynaptic inhibition from Golgi cells and disynaptic excitation from granule cells arrive simultaneously ($\Delta t = 0.1 \pm 0.3$ ms, $n = 11$, $p = 0.8$; Figure 8D). This is very different from the timing of excitation and inhibition for Purkinje cells (Figure 8E). IPSCs evoked by ChR2 activation of the MFs arrived onto Purkinje cells approximately 2 ms after a granule cell-mediated EPSC ($\Delta t = 1.8 \pm 0.3$, $n = 12$, $p < 0.001$), similar to what has been demonstrated previously with electrical stimulation of the parallel fibers (Mittmann et al., 2005). This delay defines a temporal window for summating granule cell inputs to Purkinje cells (Mittmann et al., 2005). For Golgi cells, such a window clearly does not exist, and inhibition is temporally matched with granule cell excitation. Hence, the inhibitory circuit between Golgi cells described here is quite different from the inhibitory circuits regulating Purkinje cells and does not establish a classic timing window for summation of granule cell excitation.

To determine how the timing of Golgi cell inhibition regulates their excitability following an incoming mossy fiber input to the cerebellar cortex, we again utilized dynamic clamp. In these experiments, we delivered an excitatory postsynaptic conductance (EPSG) comprised of sequential MF and granule cell EPSCs that mimic those recorded during ChR2 activation of the mossy fibers (Figure 8F). By increasing the size of this excitatory input in a stepwise manner, we determined the threshold for producing an action potential in a recorded Golgi cell. We then delivered a fixed-amplitude IPSG corresponding to a typically sized Golgi cell IPSC by using the timing that we previously measured for Golgi cell inhibition. When inhibition onto Golgi cells was properly timed, it significantly increased the threshold stimulation required for generating action potentials. However, when inhibition arrived just 2 ms later, it had no significant effect on the threshold level of excitation required for spiking the Golgi cells (Figure 8G). Hence, we find that Golgi cell feedforward inhibition has a powerful role in regulating the excitability of these cells, which would not be possible if the inhibition came from MLIs.

DISCUSSION

Here we find that, contrary to the accepted view of cerebellar cortical circuitry, Golgi cells receive synaptic inhibition from other Golgi cells and are not inhibited by MLIs. This circuit revision changes our view of how incoming mossy fiber activity is processed by the cerebellar cortex. First, the lack of either chemical or electrical synapses between MLIs and Golgi cells demonstrates that Golgi cell spiking, and hence the excitability of the entire granule cell layer, is not regulated by MLI activity. Second, because Golgi cells receive synaptic inhibition that arrives 2 ms before inhibition onto Purkinje cells, these two cell types can differentially process shared granule cell inputs.

Evidence Supporting a Revised Circuit

Multiple lines of evidence establish that Golgi cells inhibit other Golgi cells. First, following MF activation, Golgi cells and granule cells are inhibited at the same time, whereas Purkinje cells are inhibited 2 ms later. This timing is consistent with Golgi cells inhibiting one another, because granule cells are inhibited exclusively by Golgi cells, and Purkinje cells are inhibited

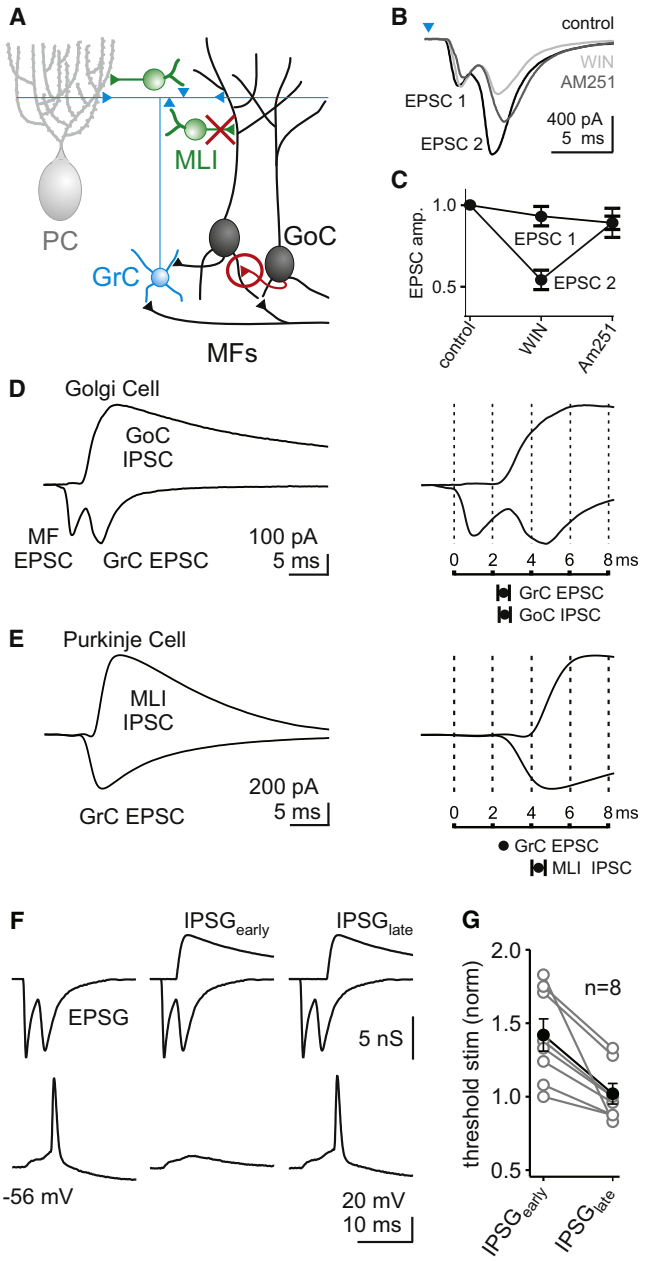

Figure 8. The Timing of Golgi Cell Inhibition Matches the Timing of Granule Cell Excitation

(A) Schematic depicting our revision of the cerebellar circuit diagram. Golgi cells make GABAergic inhibitory synapses onto each other (red circle), and MLIs do not make synapses onto Golgi cells (red X).

(B) Light activation (0.2 ms, 473 nm) evoked an excitatory current onto a Golgi cell with two distinct components (EPSC1 and EPSC2) in control (black). EPSC2 was reduced in the presence of the type 1 cannabinoid receptor (CB1R) agonist WIN (3 μM; light gray) and recovered by the additional application of the CB1R antagonist AM251 (3 μM; dark gray).

(C) The effects of the CB1R agonist and antagonist on EPSC1 and EPSC2 are summarized, and each component is normalized to its initial value in control conditions.

(D) Left: example Golgi cell recording in which the same light stimulus produces a dual component EPSC at the IPSC reversal potential and a disynaptic IPSC at the EPSC reversal potential. Right, top: the same recording on an expanded timescale shows that the onset of EPSC2 (GrC EPSC) closely matches the onset of the Golgi cell-mediated IPSC. Right, bottom: on average, the GrC excitation begins at the same time as Golgi cell-mediated inhibition (delay = 0.1 ms; n = 11).

(E) Left: a similar experiment as in (D) is shown but while recording from a Purkinje cell. Note that the EPSC onto the Purkinje cell only has one component (from the GrCs). Right, top: same recording on an expanded timescale, with the GrC EPSC set to the timing of the GrC EPSC from (D). Right, bottom: on average, the GrC excitation precedes the inhibition from MLIs (delay = 1.8 ms; n = 12).

(F) An example of a dynamic-clamp experiment that tests the function of Golgi cell inhibition and the importance of the timing of this inhibition. The timing and amplitudes of synaptic conductances were based on light-activated responses as in (D). Excitatory inputs consisted of an initial mossy fiber component followed by a granule cell component. In the absence of inhibition, this combined input could evoke action potentials for a threshold level stimulus (left). In this regime, properly timed inhibition robustly suppressed spiking (middle). If the inhibition was delayed, as it would be if it resulted from MLI synapses, the inhibition would fail to suppress spiking (right).

(G) Experiments were performed in which the size of the EPSG was varied to determine the threshold for triggering a spike. This was repeated in the presence of properly timed inhibition ($IPSG_{early}$) and late inhibition ($IPSG_{late}$). The effects of inhibition on threshold are summarized by normalizing to the level of threshold stimulus measured in the absence of inhibition. Individual experiments (open circles) and averages (closed circles) are shown.

primarily by MLIs. Second, activating mGluR2 with APDC to hyperpolarize Golgi cells reduces inhibition onto Golgi cells without significantly affecting inhibition onto Purkinje cells. Finally, paired recordings provide direct evidence that Golgi cells make GABAergic synapses onto each other.

Golgi cell inhibition of other Golgi cells appears to be both widespread and prominent. Electrical stimulation produced robust GABAergic inhibition in all Golgi cells tested, suggesting the likelihood that all Golgi cells are inhibited by other Golgi cells. Based on the size of GABAergic synaptic currents evoked by extracellular stimulation and the mean unitary conductance of Golgi cell inputs from paired recordings, each Golgi cell is inhibited by at least ten other Golgi cells. At present, it is not clear whether the moderate likelihood (20%) of observing synaptic connections between neighboring Golgi cells accurately represents the degree of connectivity in vivo or whether technical factors lower the connection rate in our brain slice recordings (see Experimental Procedures). It is notable that the connection probability between Golgi cells observed here is similar to what has been found for Golgi-cell-to-granule-cell inhibitory connections (26%) (Crowley et al., 2009). By comparison, interneuron networks in the neocortex can either be highly synaptically connected (e.g., fast-spiking basket cells, 20%–80% connection probability) (Galarreta and Hestrin, 1999, 2002; Gibson et al., 1999) or can exhibit very sparse synaptic connectivity (e.g., low threshold-spiking cells, such as Martinotti cells, 0%–15% connection probability) (Deans et al., 2001; Gibson et al., 1999). Reports of molecular diversity among Golgi cells (Geurts et al., 2001; Simat et al., 2007) raise the intriguing possibility that only specific subpopulations of Golgi cells are synaptically connected. There is, however, no evidence to date for such an arrangement.

Equally importantly, we have demonstrated that MLIs do not make fast inhibitory synapses or electrical connections onto

Golgi cells. No synaptic connections were seen in 124 paired recordings. In addition, ChR2 activation of large numbers of MLIs did not evoke any synaptic response in Golgi cells, suggesting that even weak or sparse synaptic connections from MLIs to Golgi cells do not exist. Given that MLIs provide such strong inhibition to other cell types with dendrites in the molecular layer (Purkinje cells and other MLIs), it is remarkable that Golgi cells are not also inhibited by MLIs. The lack of synaptic connections between MLIs and Golgi cells, despite the close proximity of MLI axons and Golgi cell dendrites, indicates that there must be some molecular mechanism preventing the formation of these synapses.

Functional Implications of Revised Circuitry

We find that even weak inhibition is sufficient to entrain Golgi cells, as long as the inputs are synchronous (Figure 5). Thus, our finding that Golgi cells and MLIs are not connected by either chemical or electrical synapses is crucial for understanding how activity in the granule cell layer is regulated. Specifically, the network activity of MLIs cannot influence the population of Golgi cells; MLIs are thus only responsible for regulating the excitability of Purkinje cells and other MLIs.

Differences in the sources of inhibition onto Golgi cells and Purkinje cells also have important implications for how these cells process granule cell inputs. Previously, Golgi cells were thought to be similar to Purkinje cells with respect to granule cell excitation and feedforward inhibition from MLIs. As a direct consequence of the Golgi-cell-to-Golgi-cell inhibition described here, the timing of inhibition onto Golgi cells and Purkinje cells is quite different. Inhibition onto Purkinje cells is produced in a feedforward manner by granule cell activation of MLIs, and, as a result, Purkinje cells are inhibited about 1–2 ms after they are excited by the granule cell parallel fibers (Mittmann et al., 2005). Consequently, there is a brief temporal window in which coincident granule cell activity can summate to generate precisely timed Purkinje cell spiking (Mittmann et al., 2005). Though this basic role of feedforward inhibition in controlling spike timing is common in cortical circuits (Gabernet et al., 2005; Mittmann et al., 2005; Pouille and Scanziani, 2001; Wehr and Zador, 2003), the inhibitory circuit regulating granule cell activation of Golgi cells described here is arranged quite differently.

For Golgi cells, MF activation produces disynaptic inhibition from other Golgi cells that arrives simultaneously with disynaptic excitation from the granule cells. With no delay between the onset of inhibition and granule cell excitation in Golgi cells, inhibition cannot enforce a classical integration time window for granule cell inputs. This suggests that Golgi cell spiking evoked by granule cell activity in vivo is unlikely to be precisely timed. Instead, the simultaneous Golgi cell IPSC and granule cell EPSC should generate a net potential that scales with the bulk level of excitation in the circuit and effectively reduces the amplitude of granule cell excitation. Indeed, our dynamic-clamp experiments (Figures 8F and 8G) suggest that the timing of Golgi cell inhibition is well suited to restrict granule cell excitation and can significantly increase the threshold for stimulation required to spike Golgi cells in response to a combined MF-granule cell input. Hence, rather than enforcing the precise timing of Golgi cell activation with respect to the granule cells, Golgi cell inhibition may act to limit the influence of feedback excitation. This circuit arrangement may also help to explain the observation that when a region of the cerebellar cortex is activated in vivo, Golgi cells along a beam of parallel fibers are not activated as synchronously as would be expected, given a common excitatory input (Maex et al., 2000).

In contrast to granule cell excitation, Golgi cell inhibition occurs slightly after MF excitation, suggesting that it can establish a temporal window for integrating MF inputs. Previous studies have shown that approximately four MF inputs are needed to trigger a Golgi cell spike (Kanichay and Silver, 2008), and based on the latency of inhibition, these inputs would need to arrive within approximately 2 ms. In fact, because Golgi cells and granule cells are inhibited at the same time, inhibition should play a similar role in controlling the integration of MF inputs at these two cell types.

Given the extensive characterization of cerebellar anatomy and physiology and the importance of Golgi cells to cerebellar function, it is surprising that the inhibitory circuit regulating this central interneuron has been misidentified for so long. With this revised understanding of Golgi cell connectivity, it will be possible to reexamine models of granule cell layer inhibition in response to MF inputs (Albus, 1971; Marr, 1969; Medina et al., 2000) and thus shed new light on how inhibition contributes to information processing at the input stage of the cerebellar cortex.

EXPERIMENTAL PROCEDURES

Slices

Acute slices (250–300 μm thick) were prepared from the cerebellar vermis of postnatal day (P)17–20 Sprague Dawley rats, P19–29 Thy1-ChR2/EYFP line 18 mice (Jackson Laboratory) (Arenkiel et al., 2007), and Prv-mhChR2/EYFP mice (Jackson Laboratory) (Zhao et al., 2011). Sagittal slices were used for all experiments, except for those requiring PF electrical stimulation (Figure 3B), which utilized transverse slices. All experiments requiring ChR2 activation were conducted in slices from Thy1-ChR2/EYFP and Prv-mhChR2/EYFP mice, and all other experiments were conducted in slices from rats that were of higher quality. Slices were cut in an ice-cold solution (Dugué et al., 2005; Forti et al., 2006; Kanichay and Silver, 2008) consisting of 130 mM K-gluconate, 15 mM KCl, 0.05 mM EGTA, 20 mM HEPES, and 25 mM glucose (pH 7.4) with NaOH and were then stored in a submerged chamber with artificial cerebral spinal fluid equilibrated with 95% O_2 and 5% CO_2, consisting of 125 mM NaCl, 26 mM $NaHCO_3$, 1.25 mM NaH_2PO_4, 2.5 mM KCl, 1 mM $MgCl_2$, 2 mM $CaCl_2$, and 25 mM glucose (pH 7.3, osmolarity 310). Slices were incubated initially at 34°C for 25 min and then at room temperature prior to recording. The NMDAR antagonist *R*-CPP (2.5 μM) was added to the cutting and storage solutions to enhance Golgi cell survival.

Recordings

Visually guided (infrared differential interference contrast videomicroscopy and water-immersion 40× objective) whole-cell recordings were obtained with patch pipettes (2–6 MΩ) pulled from borosilicate capillary glass (World Precision Instruments [WPI]) with a Sutter P-97 horizontal puller. Electrophysiological recordings were performed at 31°C–33°C. Slices were used within 2 hr of cutting, because synaptic inhibition onto these cells was most readily observed in fresh slices, and Golgi cells tend to die quickly in vitro.

IPSCs were recorded at the EPSC reversal potential, and EPSCs were recorded at the IPSC reversal potential, except in paired recordings and Figures 1B and 1C, in which NBQX and CPP were used to block excitation. For experiments recorded at the EPSC reversal potential, the internal pipette solution contained 140 mM Cs-methanesulfonate, 15 mM HEPES, 0.5 mM EGTA, 2 mM TEA-Cl, 2 mM MgATP, 0.3 mM NaGTP, 10 mM phosphocreatine-$tris_2$, and 2 mM QX 314-Cl. pH was adjusted to 7.2 with CsOH.

Membrane potentials were not corrected for the liquid-junction potential. The IPSC reversal potential for Golgi cells with our cesium internal solution was −64mV (n = 3). The EPSC reversal potential was determined in each experiment by adjusting the membrane potential until no EPSC was evident and was typically near +15mV. For paired recordings in which current clamp was necessary, the internal solution contained 150 mM K-gluconate, 3 mM KCl, 10 mM HEPES, 0.5 mM EGTA, 3 mM MgATP, 0.5 mM GTP, 5 mM phosphocreatine-tris$_2$, and 5 mM phosphocreatine-Na$_2$. pH was adjusted to 7.2 with NaOH. For some paired recordings, a high Cl^- potassium internal solution was used to increase the driving force for IPSCs (20 of 50 directions in 4 mM external calcium for Golgi-to-Golgi cell pairs and 31 of 60 directions in 4 mM external calcium for MLI-to-Golgi-cell pairs). In this internal solution, K-gluconate was replaced with KCl. The IPSC reversal potential was −85mV for the low Cl^- potassium internal solution (n = 3) and +4mV for the high Cl^- potassium internal (calculated). When converting to conductance values, the direction of the IPSC driving force was defined as a positive conductance. All drugs were purchased from Sigma-Aldrich or Tocris Bioscience. Paired recordings were only attempted for cells whose somata were within approximately 100 μm.

The modest synaptic connectivity rate between Golgi cells observed here (20%) may result from preferential recording from Golgi cells near the surface of the slice. Because visibility and therefore cell identification are limited deeper within the extremely dense granule cell layer, our recordings were preferentially made from superficial Golgi cells, and this may exacerbate the common problem of severing axonal arborizations in a slice preparation. Indeed, in many instances, our fluorescent fills of Golgi cells revealed that all or part of their axon was missing. Other possible factors that could affect the connection probability reported here include a selection bias toward recording from nearby Golgi cells, though the Golgi cell axon can spread more than a millimeter in the sagittal plane (Barmack and Yakhnitsa, 2008).

Data Acquisition and Analysis

Electrophysiolgical data were acquired using a multiclamp 700B amplifier (Axon Instruments), digitized at 20 kHz either with a National Instruments USB-6229, a National Instruments PCI-MIO 16E-4 board, or an ITC-18 (Instrutech, Great Neck, NY), and filtered at 2 kHz. Acquisition was controlled both with custom software written either in MATLAB (generously provided by Bernardo Sabatini, Harvard Medical School, Boston, MA), or IgorPro (generously provided by Matthew Xu-Friedman, SUNY Buffalo, Buffalo, NY). Series resistance was monitored in voltage-clamp recordings with a 5mV hyperpolarizing pulse, and only recordings that remained stable over the period of data collection were used. Glass monopolar electrodes (1–2 MΩ) filled with artificial cerebral spinal fluid in conjunction with a stimulus isolation unit (WPI, A360) were used for extracellular stimulation. EPSC and IPSC latencies were determined by their 5% rise time, except in Figure 6, in which the peak of the second derivative was used (negative peaks for EPSCs, positive peak for IPSCs). Data are reported as mean ± SEM, and statistical analysis was carried out using the two-tailed Student's t test. For all experiments involving APDC and WIN, the percentage of IPSC reduction is measured relative to the average of control and recovery (or antagonist) conditions.

ChR2 Stimulation

Slices from Thy1-ChR2/EYFP and Prv-mhChR2/EYFP mice were stored in the dark. A 473 nm blue laser was used to stimulate ChR2 (Opto Engine, Midvale, UT). In the Thy1-ChR2 mice, excitation and inhibition were evoked using full-field illumination with either a low-intensity (<1 mW under the objective) stimulus for 1–5 ms or a high-intensity stimulus (1–10 mW under the objective) for 0.2 ms. Although both regimes were capable of producing a compound MF-granule cell response in Thy1-ChR2 mice, the shorter, high-intensity stimulation more effectively separated these components, presumably by generating only brief activity in the MFs. MFs were stimulated at 0.1 Hz. Evoked responses typically ran down with time (as in Figures 3A and 6C) at the rate of approximately 7% in 10 min. In the Prv-mhChR2/EYFP experiments (Figure 7), MLIs were also stimulated at 0.1 Hz using full-field illumination. Based on the mean unitary conductance of MLI→PC synapses (0.4 nS), the mean inhibitory conductance evoked onto PCs in these experiments (12.6 nS), and the 60% connectivity between MLIs and PCs (Figure 6), we estimate that an average of ~50 MLIs was activated by ChR2 in each paired recording (average = [12.6 nS / 0.4 nS] / 0.6).

Dynamic Clamp

Dynamic-clamp recordings were made using the built-in dynamic-clamp mode of the ITC-18. The AMPA receptor (AMPAR) conductance simulating a combined MF and granule cell EPSC (Figure 8) was constructed by adding a recorded MF EPSC with a recorded granule cell EPSC from electrical simulation to mimic the EPSCs evoked by ChR2 stimulation of the MFs. The IPSG waveform was taken from a recorded Golgi cell IPSC in response to electrical stimulation (Figure 1) and was used for both spike-entrainment experiments (Figure 5) and timing experiments (Figure 8). AMPAR conductances reversed at 0mV, whereas inhibitory conductances reversed at −75mV. Dynamic-clamp recordings were performed in the presence of NBQX (5 μM), CPP (2.5 μM), gabazine (5 μM), and CGP (1 μM). Cells were allowed to rest at their normal potential and spike spontaneously without any injected current. For timing experiments, injected conductances were spike triggered and timed to occur 100 ms after a spontaneous spike when the afterhyperpolarization was completed.

Two-Photon Imaging

Neurons were filled with either 50 μM Alexa 594 hydrazide or 75 μM Alexa 488 hydrazide for two-photon imaging and morphological characterization. Cells were imaged using a custom two-photon laser scanning microscope that used 800 nm illumination. Images were processed in either ImageJ or Photoshop by adjusting the contrast, brightness, and image noise. For cells in which multiple stacks were taken to encompass the entirety of two filled cells, images were aligned by eye.

SUPPLEMENTAL INFORMATION

Supplemental Information includes five figures and can be found with this article online at doi:10.1016/j.neuron.2011.10.030.

ACKNOWLEDGMENTS

Work was supported by National Institutes of Health grants R37 NS032405 to W.G.R. and F32 NS060585 to C.H.

Accepted: October 10, 2011
Published: January 11, 2012

REFERENCES

Albus, J.S. (1971). A theory of cerebellar function. Math. Biosci. *10*, 25–61.

Arenkiel, B.R., Peca, J., Davison, I.G., Feliciano, C., Deisseroth, K., Augustine, G.J., Ehlers, M.D., and Feng, G. (2007). In vivo light-induced activation of neural circuitry in transgenic mice expressing channelrhodopsin-2. Neuron *54*, 205–218.

Atallah, B.V., and Scanziani, M. (2009). Instantaneous modulation of gamma oscillation frequency by balancing excitation with inhibition. Neuron *62*, 566–577.

Barmack, N.H., and Yakhnitsa, V. (2008). Functions of interneurons in mouse cerebellum. J. Neurosci. *28*, 1140–1152.

Barmack, N.H., Baughman, R.W., and Eckenstein, F.P. (1992a). Cholinergic innervation of the cerebellum of rat, rabbit, cat, and monkey as revealed by choline acetyltransferase activity and immunohistochemistry. J. Comp. Neurol. *317*, 233–249.

Barmack, N.H., Baughman, R.W., Eckenstein, F.P., and Shojaku, H. (1992b). Secondary vestibular cholinergic projection to the cerebellum of rabbit and rat as revealed by choline acetyltransferase immunohistochemistry, retrograde and orthograde tracers. J. Comp. Neurol. *317*, 250–270.

Beierlein, M., Fioravante, D., and Regehr, W.G. (2007). Differential expression of posttetanic potentiation and retrograde signaling mediate target-dependent short-term synaptic plasticity. Neuron *54*, 949–959.

Cobb, S.R., Buhl, E.H., Halasy, K., Paulsen, O., and Somogyi, P. (1995). Synchronization of neuronal activity in hippocampus by individual GABAergic interneurons. Nature *378*, 75–78.

Crowley, J.J., Fioravante, D., and Regehr, W.G. (2009). Dynamics of fast and slow inhibition from cerebellar golgi cells allow flexible control of synaptic integration. Neuron *63*, 843–853.

D'Angelo, E. (2008). The critical role of Golgi cells in regulating spatio-temporal integration and plasticity at the cerebellum input stage. Front Neurosci. *2*, 35–46.

D'Angelo, E., and De Zeeuw, C.I. (2009). Timing and plasticity in the cerebellum: focus on the granular layer. Trends Neurosci. *32*, 30–40.

De Schutter, E., Vos, B., and Maex, R. (2000). The function of cerebellar Golgi cells revisited. Prog. Brain Res. *124*, 81–93.

Deans, M.R., Gibson, J.R., Sellitto, C., Connors, B.W., and Paul, D.L. (2001). Synchronous activity of inhibitory networks in neocortex requires electrical synapses containing connexin36. Neuron *31*, 477–485.

Dieudonné, S., and Dumoulin, A. (2000). Serotonin-driven long-range inhibitory connections in the cerebellar cortex. J. Neurosci. *20*, 1837–1848.

Dugué, G.P., Dumoulin, A., Triller, A., and Dieudonné, S. (2005). Target-dependent use of co-released inhibitory transmitters at central synapses. J. Neurosci. *25*, 6490–6498.

Dugué, G.P., Brunel, N., Hakim, V., Schwartz, E., Chat, M., Lévesque, M., Courtemanche, R., Léna, C., and Dieudonné, S. (2009). Electrical coupling mediates tunable low-frequency oscillations and resonance in the cerebellar Golgi cell network. Neuron *61*, 126–139.

Dumoulin, A., Triller, A., and Dieudonné, S. (2001). IPSC kinetics at identified GABAergic and mixed GABAergic and glycinergic synapses onto cerebellar Golgi cells. J. Neurosci. *21*, 6045–6057.

Eccles, J., Llinas, R., and Sasaki, K. (1964). Golgi cell inhibition in the cerebellar cortex. Nature *204*, 1265–1266.

Eccles, J.C., Llinás, R., and Sasaki, K. (1966). The inhibitory interneurones within the cerebellar cortex. Exp. Brain Res. *1*, 1–16.

Eccles, J., Ito, M., and Szentágothai, J. (1967). The Cerebellum as a Neuronal Machine (Berlin: Springer).

Forti, L., Cesana, E., Mapelli, J., and D'Angelo, E. (2006). Ionic mechanisms of autorhythmic firing in rat cerebellar Golgi cells. J. Physiol. *574*, 711–729.

Gabernet, L., Jadhav, S.P., Feldman, D.E., Carandini, M., and Scanziani, M. (2005). Somatosensory integration controlled by dynamic thalamocortical feed-forward inhibition. Neuron *48*, 315–327.

Galarreta, M., and Hestrin, S. (1999). A network of fast-spiking cells in the neocortex connected by electrical synapses. Nature *402*, 72–75.

Galarreta, M., and Hestrin, S. (2002). Electrical and chemical synapses among parvalbumin fast-spiking GABAergic interneurons in adult mouse neocortex. Proc. Natl. Acad. Sci. USA *99*, 12438–12443.

Galliano, E., Mazzarello, P., and D'Angelo, E. (2010). Discovery and rediscoveries of Golgi cells. J. Physiol. *588*, 3639–3655.

Geurts, F.J., Timmermans, J., Shigemoto, R., and De Schutter, E. (2001). Morphological and neurochemical differentiation of large granular layer interneurons in the adult rat cerebellum. Neuroscience *104*, 499–512.

Geurts, F.J., De Schutter, E., and Dieudonné, S. (2003). Unraveling the cerebellar cortex: cytology and cellular physiology of large-sized interneurons in the granular layer. Cerebellum *2*, 290–299.

Gibson, J.R., Beierlein, M., and Connors, B.W. (1999). Two networks of electrically coupled inhibitory neurons in neocortex. Nature *402*, 75–79.

Grüsser-Cornehls, U., and Bäurle, J. (2001). Mutant mice as a model for cerebellar ataxia. Prog. Neurobiol. *63*, 489–540.

Häusser, M., and Clark, B.A. (1997). Tonic synaptic inhibition modulates neuronal output pattern and spatiotemporal synaptic integration. Neuron *19*, 665–678.

Isope, P., Dieudonné, S., and Barbour, B. (2002). Temporal organization of activity in the cerebellar cortex: a manifesto for synchrony. Ann. N Y Acad. Sci. *978*, 164–174.

Ito, M. (2006). Cerebellar circuitry as a neuronal machine. Prog. Neurobiol. *78*, 272–303.

Jaarsma, D., Ruigrok, T.J., Caffé, R., Cozzari, C., Levey, A.I., Mugnaini, E., and Voogd, J. (1997). Cholinergic innervation and receptors in the cerebellum. Prog. Brain Res. *114*, 67–96.

Jörntell, H., Bengtsson, F., Schonewille, M., and De Zeeuw, C.I. (2010). Cerebellar molecular layer interneurons - computational properties and roles in learning. Trends Neurosci. *33*, 524–532.

Kanichay, R.T., and Silver, R.A. (2008). Synaptic and cellular properties of the feedforward inhibitory circuit within the input layer of the cerebellar cortex. J. Neurosci. *28*, 8955–8967.

Kerr, C.W., and Bishop, G.A. (1991). Topographical organization in the origin of serotoninergic projections to different regions of the cat cerebellar cortex. J. Comp. Neurol. *304*, 502–515.

Kistler, W.M., and De Zeeuw, C.I. (2003). Time windows and reverberating loops: a reverse-engineering approach to cerebellar function. Cerebellum *2*, 44–54.

Maex, R., Vos, B.P., and De Schutter, E. (2000). Weak common parallel fibre synapses explain the loose synchrony observed between rat cerebellar golgi cells. J. Physiol. *523*, 175–192.

Mann, E.O., Suckling, J.M., Hajos, N., Greenfield, S.A., and Paulsen, O. (2005). Perisomatic feedback inhibition underlies cholinergically induced fast network oscillations in the rat hippocampus in vitro. Neuron *45*, 105–117.

Mapelli, L., Rossi, P., Nieus, T., and D'Angelo, E. (2009). Tonic activation of GABAB receptors reduces release probability at inhibitory connections in the cerebellar glomerulus. J. Neurophysiol. *101*, 3089–3099.

Marr, D. (1969). A theory of cerebellar cortex. J. Physiol. *202*, 437–470.

Mauk, M.D., Medina, J.F., Nores, W.L., and Ohyama, T. (2000). Cerebellar function: coordination, learning or timing? Curr. Biol. *10*, R522–R525.

Medina, J.F., Garcia, K.S., Nores, W.L., Taylor, N.M., and Mauk, M.D. (2000). Timing mechanisms in the cerebellum: testing predictions of a large-scale computer simulation. J. Neurosci. *20*, 5516–5525.

Mitchell, S.J., and Silver, R.A. (2000). GABA spillover from single inhibitory axons suppresses low-frequency excitatory transmission at the cerebellar glomerulus. J. Neurosci. *20*, 8651–8658.

Mittmann, W., Koch, U., and Häusser, M. (2005). Feed-forward inhibition shapes the spike output of cerebellar Purkinje cells. J. Physiol. *563*, 369–378.

Ohishi, H., Ogawa-Meguro, R., Shigemoto, R., Kaneko, T., Nakanishi, S., and Mizuno, N. (1994). Immunohistochemical localization of metabotropic glutamate receptors, mGluR2 and mGluR3, in rat cerebellar cortex. Neuron *13*, 55–66.

Palay, S., and Chan-Palay, V. (1974). Cerebellar Cortex (New York: Springer).

Pouille, F., and Scanziani, M. (2001). Enforcement of temporal fidelity in pyramidal cells by somatic feed-forward inhibition. Science *293*, 1159–1163.

Simat, M., Parpan, F., and Fritschy, J.-M. (2007). Heterogeneity of glycinergic and gabaergic interneurons in the granule cell layer of mouse cerebellum. J. Comp. Neurol. *500*, 71–83.

Sotelo, C., and Llinás, R. (1972). Specialized membrane junctions between neurons in the vertebrate cerebellar cortex. J. Cell Biol. *53*, 271–289.

Vervaeke, K., Lőrincz, A., Gleeson, P., Farinella, M., Nusser, Z., and Silver, R.A. (2010). Rapid desynchronization of an electrically coupled interneuron network with sparse excitatory synaptic input. Neuron *67*, 435–451.

Watanabe, D., and Nakanishi, S. (2003). mGluR2 postsynaptically senses granule cell inputs at Golgi cell synapses. Neuron *39*, 821–829.

Watanabe, D., Inokawa, H., Hashimoto, K., Suzuki, N., Kano, M., Shigemoto, R., Hirano, T., Toyama, K., Kaneko, S., Yokoi, M., et al. (1998). Ablation of cerebellar Golgi cells disrupts synaptic integration involving GABA inhibition and NMDA receptor activation in motor coordination. Cell *95*, 17–27.

Wehr, M., and Zador, A.M. (2003). Balanced inhibition underlies tuning and sharpens spike timing in auditory cortex. Nature *426*, 442–446.

Zhao, S., Ting, J.T., Atallah, H.E., Qiu, L., Tan, J., Gloss, B., Augustine, G.J., Deisseroth, K., Luo, M., Graybiel, A.M., and Feng, G. (2011). Cell type–specific channelrhodopsin-2 transgenic mice for optogenetic dissection of neural circuitry function. Nat. Methods *8*, 745–752.